

Orientation of Surface-Active Azodye in Langmuir-Blodgett Films as Determined by IR and UV-Visible Spectroscopies

Toyoko IMAE*1,*2 and Hiroyuki TORII*2

*1 Research Center for Materials Science and

*2 Graduate School of Science,

Nagoya University (Chikusa-ku, Nagoya-shi, Aichi-ken 464-8602)

Abstract : Infrared (IR) transmission and reflection-absorption spectra were measured for Langmuir-Blodgett (LB) films of surface-active azodye prepared at surface pressures of 5 and 30 mNm⁻¹. The IR spectra showed that the molecules are preferentially arranged in the LB films with the molecular orientation dependent on the transfer pressure. The absorption peak of the trans isomer of the azodye in the ultraviolet-visible absorption spectra blue-shifted for the LB film prepared at 5 mNm⁻¹ and red-shifted for that at 30 mNm⁻¹. The formation of H and J aggregates of the azodye, respectively, would thus appear to occur. The orientation of the azodye molecules in the LB films is discussed.

Key words : surface-active azodye, azobenzene derivative, Langmuir-Blodgett film, infrared reflection-absorption spectrum, H aggregate, J aggregate

1 Introduction

Azodyes are useful for indicators, dyestuffs, and other industrial applications^{1,2}. Moreover, the development of photochromic liquid crystal display, photoswitching, and energy transfer devices is projected, in connection with organizing property of dyes. For those purposes, amphiphilic azodyes³⁻⁸ and polymers with azodye side or main chains^{9,10-11} are synthesized besides simple azodye derivatives¹²⁻¹⁶. Thin films on substrates such as cast, deposit, spin-coat, Langmuir-Blodgett (LB), and self-assembled monolayer films have been investigated by using spectroscopy^{3-6,8-14,16-19}, surface tensiometry^{5,11}, X-ray diffraction^{6,12}, atomic force microscopy (AFM)^{7,8,12-14}, Brewster angle microscopy¹¹, cyclic voltammetry^{12,15}, ellipsometry¹², surface plasmon resonance¹⁶, and so on.

A non-ionic surface-active azodye, *p*-tert-octylphenol yellow amine poly(ethylene oxide) (YOPE) (see **Chart 1**), consists of a hydrophilic part and a hydrophobic part linked by an azobenzene group²⁰⁻²⁴. YOPE is insoluble in water but forms micelles in dilute, aqueous methanol solutions, followed by lyotropic liquid

crystal formation in more concentrated solutions. Two-dimensional organization of YOPE has been achieved by constructing Langmuir and LB films. AFM observations revealed that the morphology of the LB films depends on the transfer pressure, indicating that the transfer pressure affected molecular arrangement in the films²⁴. However, the precise molecular arrangement was not determined in the preceding paper.

In the present work, LB films of YOPE prepared at different surface pressures are examined by infrared (IR) and ultraviolet (UV)-visible spectroscopies, and the orientation of YOPE in the films is discussed by referring to the model based on the AFM observations²⁴.

2 Experimental

2.1 Chemicals

The YOPE sample was the same as that previously used²⁰⁻²⁴. Water was purified by a MILLI-Q Labo (Millipore). Other reagents were commercially available.

2.2 Surface Tensiometric Measurement and LB Film Preparation

Surface tensiometric measurement and LB film preparation were performed on a LB film deposition apparatus (Nippon Laser & Electronics Lab, Nagoya) with a trough maintained at 25 °C.

Corresponding author : Toyoko IMAE

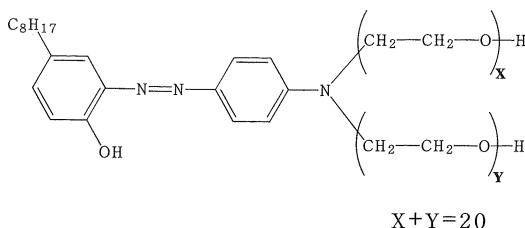


Chart 1 Chemical Structure of YOPE.

Details of the procedure are described elsewhere²⁴. Langmuir monolayer films were transferred onto substrates by the upstroke mode of the dipping method. Substrates used are CaF₂, Au (200 nm thickness)-evaporated glass (pre-evaporated by Cr (150 nm thickness)), and quartz substrates were used for IR transmission, IR reflection-absorption (RA), and UV-visible absorption spectroscopic measurements, respectively.

2.3 Spectroscopic Measurements

IR spectra were recorded with a Bio-Rad FTS 575C FT-IR Spectrometer equipped with a liquid nitrogen-cooled mercury-cadmium-telluride (MCT) detector. Interferograms were accumulated 1024 times at 4 cm⁻¹ resolution. RA spectra were taken using a Harrick reflectance attachment with a 75° incidence angle. UV-visible spectra were measured on a Shimadzu UV-2200 Spectrophotometer. All measurements were carried out at room temperature (~25 °C).

3 Results

3.1 Surface Pressure-surface Area (π -A) Isotherm

Figure 1 shows the π -A isotherm of YOPE Langmuir monolayer. During compression of the monolayer, the surface pressure gradually increased at surface areas below 150 Å²molecule⁻¹, and the monolayer was destroyed at a surface pressure of 50 mNm⁻¹ or at an occupied area of 50 Å²molecule⁻¹. The large occupied area per YOPE molecule, in comparison with that of the azodye with a single alkyl chain^{5,11}, indicates the expanded arrangement of YOPE due to the bulky head and tail groups. The π -A isotherm profile obtained is consistent with the previously reported one²⁴. LB films were prepared at surface pressures of 5 and 30 mNm⁻¹, where occupied areas per molecule were 120 and 90 Å²molecule⁻¹, respectively.

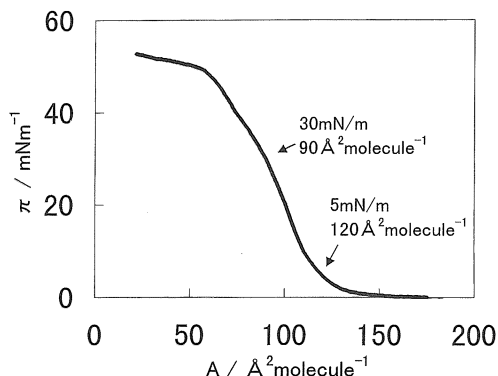


Fig. 1 Surface Pressure-surface Area Isotherm of YOPE Langmuir Monolayer.

3.2 IR Absorption Spectra

IR transmission and RA spectra of LB monolayer films prepared at 5 and 30 mNm⁻¹ are illustrated in Figs. 2 and 3. Band positions are listed in Table 1, which includes band assignments according to the literatures^{5,14,25}. IR transmission spectrum was also measured for oily YOPE deposited on a CaF₂ window, and their band positions are included in Table 1. Although IR transmission and RA spectra for deposit and LB films were similar to each other, some of the band positions and their relative intensities were different. A broad OH stretching band was

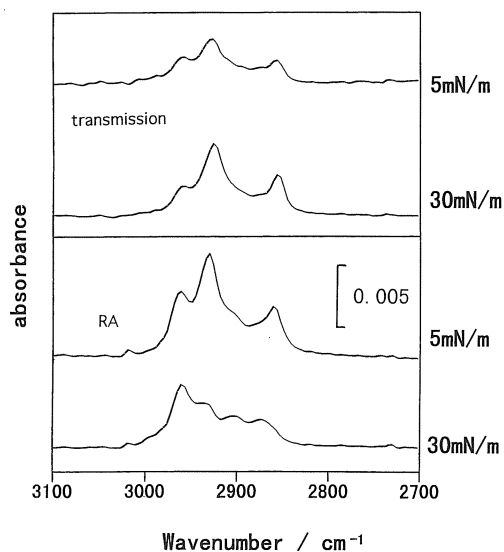


Fig. 2 IR Transmission and RA Spectra, in the Region of 3100~2700 cm⁻¹, of YOPE LB Monolayer Films Prepared at 5 and 30 mNm⁻¹.

Table 1 Band Positions (cm^{-1}) and Their Assignments for Infrared Absorption Spectra of Surface-Active Azodye in LB Films^{a)}.

deposit film	transmission		RA		band assignment
	LB film at		LB film at		
	5mNm ⁻¹	30mNm ⁻¹	5mNm ⁻¹	30mNm ⁻¹	
3 353m	~ 3 345br	~ 3 345br	w	w	hydrogen-bonded OH stretch
2 952m	2 957m	2 958m	2 960m	2 960s	CH ₃ asym stretch
2 920s	2 926s	2 925s	2 930s	2 935m	CH ₂ antisym stretch
2 871m	2 875sh	2 875sh	2 871sh	2 872m	CH ₃ sym stretch
2 852m	2 856m	2 855m	2 859m	2 857sh	CH ₂ sym stretch
1 601s	1 601m	1 601m	1 601m	1 601m	ring c-c stretch ip (ν_{8a})
1 504m	1 504w	1 501w	1 504m	1 505m	ring c-c stretch ip (ν_{19a})
1 455m	1 455w	1 455w	1 459m	1 455m	CH ₂ scissor
1 366w	1 366w	1 366w	1 366m	1 366m	CH ₂ wag
1 253m	1 258w	1 260w	1 252m	1 252m	ring CH bend ip

^{a)}s, strong ; m, medium ; w, weak ; sh, shoulder ; br, broad ; ip, in-plane

observed at 3353 cm^{-1} in the deposit film. The band, which is assigned to hydrogen-bonded state, was slightly weak in IR transmission spectra of LB films in comparison with CH₃ and CH₂ stretching vibration bands in the region of $3000\sim 2800\text{ cm}^{-1}$. This feature is more pronounced in the IR-RA spectra. This implies that the OH axis is oriented in the LB films.

The intensities of CH₂ antisymmetric and symmetric stretching bands were stronger than

those of the CH₃ asymmetric and symmetric bands for the deposit film. Similar features were observed in both transmission and RA spectra for the LB film transferred at 5 mNm^{-1} . For the LB film prepared at 30 mNm^{-1} , the CH₂ band intensities in the IR transmission spectrum were stronger than the CH₃ band intensities, whereas the relative intensities were opposite in the IR-RA spectrum, indicating that the molecular orientation of the LB film prepared at 30 mNm^{-1} is different from that at 5 mNm^{-1} .

The 1455 and 1366 cm^{-1} bands are assigned to CH₂ scissoring and wagging bands, respectively, and the 1601 , 1504 , and 1253 cm^{-1} bands are due to in-plane ring C-C stretching and CH bending modes. The vibration band at 1601 cm^{-1} was stronger than the other bands in the deposit film but comparable in intensity to the other bands in the LB films, especially in the IR-RA spectra. This indicates that YOPE molecules are in oriented arrangement in the LB films.

3.3 UV-visible Absorption Spectra

A UV-visible spectrum of YOPE in chloroform is given in Fig. 4. The absorption peak at 387 nm , which is assigned to $\pi\text{-}\pi^*$ transition with the electronic transition moment parallel to the long axis of trans-azobenzene moiety¹³, was higher in wavelength than those of simple azobenzene derivatives previously reported^{8),13}. The wavelength shift originates in 4-amino substitution of azobenzene²⁶.

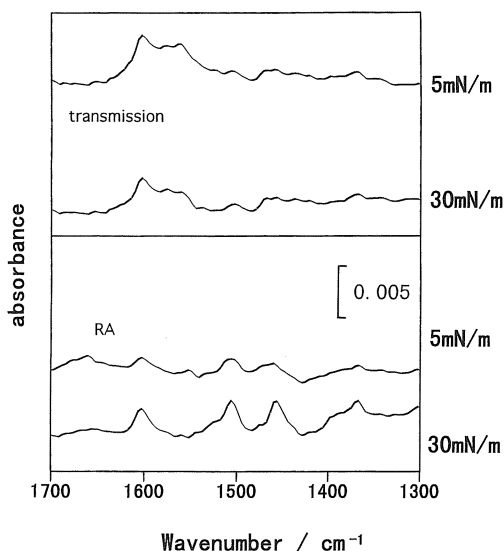


Fig. 3 IR Transmission and RA Spectra, in the Region of $1700\sim 1300\text{ cm}^{-1}$, of YOPE LB Monolayer Films Prepared at 5 and 30 mNm^{-1} .

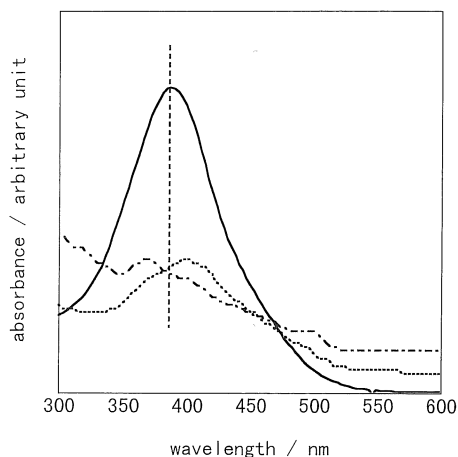


Fig. 4 UV-visible Spectra of YOPE in Chloroform and of YOPE LB Films. —, in chloroform; ---, LB film at 5 mNm⁻¹; ·····, LB film at 30 mNm⁻¹.

UV-visible spectra of the LB films prepared at 5 and 30 mNm⁻¹ exhibit absorption bands at 370 and 397 nm, respectively (Fig. 4). Blue and red shifts of the band are owing to the formation of H and J aggregates, respectively^{9,13}. Therefore, the spectrum change reflects the difference of the molecular arrangement in the LB films prepared at different surface pressures.

4 Discussion

The azobenzene derivative, YOPE molecule, consists of moieties of a *tert*-octyl chain, a 2'-hydroxy-4-aminoazobenzene, and ethylene oxide chains. IR absorption spectra give us information on molecular arrangement in the LB film, when they are compared with a spectrum of the deposit film where molecules are in the disordered state. The difference of interaction of YOPE molecule with the substrate as well as the difference of molecular orientation on the substrate causes the variation of positions and intensities of IR absorption bands between deposit film and LB films. On the other hand, the difference of surface

selection rule gives rise to a remarkable difference of band intensities²⁷. According to the selection rule of IR-RA spectroscopy, vibrations with transition moments perpendicular to the metal substrate are enhanced by the electric field normal to the substrate. On the contrary, vibrations parallel to the substrate appear in the transmission mode. It is clear from Figs. 2 and 3 that the reflection-absorption effect on Au-evaporated substrate intensifies infrared bands, although the enhancement efficiency is different from band to band.

The hydrogen-bonded OH stretching band at 3353 cm⁻¹, when it is compared with the other vibration bands, is weak in the LB films rather than in the deposit film. This effect was more pronounced in the IR-RA spectrum than in the IR transmission spectrum of the LB films. This indicates that O-H axes in ethylene oxide chains and/or an OH axis in 2'-hydroxy-4-aminoazobenzene moiety in the LB films should be parallel to the substrate. The hydrogen-bond formation of 2'-hydroxyl residue with azo nitrogen in aqueous methanol solution is confirmed from absorption spectra²¹.

Since both CH₂ antisymmetric and symmetric stretching vibration bands shift from 2920 and 2852 cm⁻¹ in the deposit film to higher wavenumbers in the LB films, ethylene oxide chains with *trans* conformation in the deposit film change to *gauche* conformers in the LB films²⁹⁻³¹. The conformation of *tert*-octyl chain may also be varied between deposit and LB films, as similar band shift was observed even for a CH₃ asymmetric stretching band. It should be noticed that the intensity ratio of CH₂ antisymmetric stretching band against CH₃ asymmetric stretching band changes for different IR modes and films, as seen in Table 2. The ratio in the IR transmission spectra increases in the order of deposit film, LB film at 5 mNm⁻¹, and LB film at 30 mNm⁻¹. Moreover, the value for the RA spectrum in LB film at 30 mNm⁻¹ is drastically different from that for the transmission spectrum.

Table 2 Intensity Ratio of CH₂ Antisymmetric Stretching Vibration Band Against CH₃ Asymmetric Stretching Vibration Band.

IR mode	deposit film	LB film at 5mNm ⁻¹	LB film at 30mNm ⁻¹
transmission	1.28	1.67	2.38
RA		1.61	0.70

This means the oriented arrangement of YOPE molecules in the LB films, at least, in the LB film prepared at 30 mNm^{-1} . Similar tendency was obtained when the intensity ratio of CH_2 symmetric stretching band against CH_3 asymmetric stretching band was compared. The increase of the ratio in the transmission spectrum and the decrease in the RA spectrum imply that the tilt angle of ethylene oxide chains and/or of a *tert*-octyl chain becomes more normal to water subphase during the compression of Langmuir monolayer.

IR band shifts in the region of $1700 \sim 1200 \text{ cm}^{-1}$ are not remarkable for all the IR modes irrespective of the film preparation method. However, the absorption band (1601 cm^{-1}) of benzene ring C-C stretching vibration mode (ν_{8a}) in azobenzene, the transition moment of which is parallel to the longer axis of azobenzene, was not strong in either IR transmission or RA spectra for LB films in comparison with CH_3 and CH_2 stretching bands. This feature is completely different from that of deposit film. This may imply that the long axis of azobenzene should be tilted on the substrate.

YOPE in chloroform displays an absorption band at 387 nm in the UV-visible absorption spectrum. Similar band position was obtained in various organic solvents²¹. The band shifts to blue and red in the LB films prepared at 5 and 30 mNm^{-1} , respectively, indicating the formation of H and J aggregates. The long axes of chromophores in H aggregate are packed parallel to each other by strong interchromophoric interaction, and those in J aggregate are arranged as in a brick stone work. YOPE moieties are stacked by side-by-side mode in the LB film prepared at 5 mNm^{-1} , whereas the moieties in the LB film prepared at 30 mNm^{-1} are rather in a head-to-tail arrangement.

Figure 5 schematically presents the orientation of YOPE molecules in the LB film on the substrate. In arrangement (a), YOPE molecules lie on the substrate and, therefore, molecular axes should be arranged accordingly. Some of YOPE molecules form H aggregate. This arrangement is formed in the LB film prepared at lower surface pressures. YOPE molecules in the arrangement (b) are tilted on the substrate and form J aggregate. According to the variation of arrangement, octyl chain, azobenzene-axis, and ethylene oxide chains gradually stand up. This situation

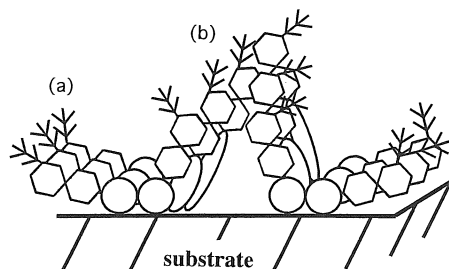


Fig. 5 Schematic Presentation of Orientation of YOPE Molecules in LB Film on Substrate.

occurs when the monolayer is compressed to high surface pressures. The profile in the present work is consistent with that obtained from AFM observation²⁴. At lower surface pressures such as 5 mNm^{-1} , YOPE molecules lie with $\sim 20 \text{ \AA}$ height on the substrate, corresponding to the arrangement (a) in Fig. 5. The rough surface at 25 mNm^{-1} consists of bumps with various height differences, 80 \AA being the maximum. In the bumps, molecules should be arranged as in the model (b). Thus, the arrangements (a) and (b) should coexist in the LB films prepared at high surface pressures.

(Received Dec. 27, 1999 ; Accepted Feb. 28, 2000)

References

- 1) C.F. Hiskey, T.A. Downey, *J. Phys. Chem.*, **58**, 835 (1954).
- 2) Y. Nemoto, H. Funahashi, *Hyomen*, **15**, 625 (1977).
- 3) (a) T. Kunitake, N. Nakashima, M. Shimomura, Y. Okahata, K. Kano, T. Ogawa, *J. Am. Chem. Soc.*, **102**, 6642 (1980). (b) T. Kunitake, Y. Okahata, M. Shimomura, S. Yasunami, K. Takarabe, *J. Am. Chem. Soc.*, **103**, 5401 (1981).
- 4) K. Fukuda, H. Nakahara, *J. Colloid Interface Sci.*, **98**, 555 (1984).
- 5) T. Sato, Y. Ozaki, K. Iriyama, *Langmuir*, **10**, 2363 (1994).
- 6) N. Yamada, K. Okuyama, T. Serizawa, M. Kawasaki, S. Oshima, *J. Chem. Soc. Perkin Trans. 2*, 2707 (1996).
- 7) T. Seki, K. Tanaka, K. Ichimura, *Macromolecules*, **30**, 6401 (1997).
- 8) M. Véléz, S. Mukhopadhyay, I. Muzikante, G. Matisova, S. Vieira, *Langmuir*, **13**, 870 (1997).
- 9) J.L. Houben, A. Fissi, D. Bacciola, N. Rosato, O. Pieroni, F. Ciardelli, *Int. J. Biol. Macromol.*, **5**, 94 (1983).
- 10) Th. Geue, A. Ziegler, J. Stumpe, *Macromolecules*, **30**, 5729 (1997).

- 11) T. Seki, H. Sekizawa, S. Morino, K. Ichimura, *J. Phys. Chem. B*, **102**, 5313 (1998).
 - 12) W.B. Caldwell, D.J. Campbell, K. Chen, B.R. Herr, C.A. Mirkin, A. Malik, M.K. Durbin, P. Dutta, K.G. Huang, *J. Am. Chem. Soc.*, **117**, 6071 (1995).
 - 13) R. Wang, T. Iyoda, L. Jiang, K. Hashimoto, A. Fujishima, *Chemistry Letters*, 1005 (1996).
 - 14) R. Wang, L. Jiang, T. Iyoda, D.A. Tryk, K. Hashimoto, A. Fujishima, *Langmuir*, **12**, 2052 (1996).
 - 15) H.Z. Yu, H.B. Shao, Y. Luo, H.L. Zhang, Z.F. Liu, *Langmuir*, **13**, 5774 (1997).
 - 16) S.D. Evans, S.R. Johnson, H. Ringsdorf, L.M. Williams, H. Wolf, *Langmuir*, **14**, 6436 (1998).
 - 17) J. Heesemann, *J. Am. Chem. Soc.*, **102**, 2167, 2176 (1980).
 - 18) D. Mobius, *Accounts Chem. Res.*, **14**, 63 (1981).
 - 19) T. Kawai, J. Umemura, T. Takenaka, *Langmuir*, **5**, 1378 (1989); **6**, 672 (1990).
 - 20) T. Imae, C. Mori, S. Ikeda, *J. Chem. Soc. Faraday Trans. 1*, **78**, 1359 (1982).
 - 21) T. Imae, C. Mori, S. Ikeda, *J. Chem. Soc. Faraday Trans. 1*, **78**, 1369 (1982).
 - 22) T. Imae, S. Ikeda, K. Itoh, *J. Chem. Soc. Faraday Trans. 1*, **79**, 2843 (1983).
 - 23) T. Imae, S. Ikeda, *Mol. Cryst. Liq. Cryst.*, **101**, 155 (1983).
 - 24) T. Imae, K. Aoki, *Langmuir*, **14**, 1196 (1998).
 - 25) M.S. Johal, A.N. Parikh, Y. Lee, J.L. Casson, L. Foster, B.I. Swanson, D.W. McBranch, D.Q. Li, J.M. Robinson, *Langmuir*, **15**, 1275 (1999).
 - 26) W.R. Brode, I.L. Seldin, P.E. Spoerri, G.M. Wyman, *J. Am. Chem. Soc.*, **77**, 2762 (1955).
 - 27) J. Umemura, T. Kamata, T. Kawai, T. Takenaka, *J. Phys. Chem.*, **94**, 62 (1990).
 - 28) H. Sapper, D.G. Cameron, H.H. Mantsch, *Can. J. Chem.*, **59**, 2543 (1981).
 - 29) T. Kamata, J. Umemura, T. Takenaka, N. Koizumi, *J. Phys. Chem.*, **95**, 4096 (1991).
 - 30) Y. Tian, *J. Phys. Chem.*, **95**, 9995 (1991).
 - 31) D.A. Myrzakozha, T. Hasegawa, J. Nishijo, T. Imae, Y. Ozaki, *Langmuir*, **15**, 6890 (1999).
-

[報文]

2,4-オクタデカジエン基を有するリン脂質と 非重合性成分からなる混合系リポソームの γ 線重合

赤間 和博^{*1}・粟井 浩二^{*1}・矢野 嘉宏^{*1}
徳山 悟^{*1}・中野 善郎^{*1}・細井 文雄^{*2}・大道 英樹^{*2}

*1 日本油脂株式会社 筑波研究所 (〒300-2635 茨城県つくば市東光台5-10)

*2 日本原子力研究所 高崎研究所 (〒370-1207 群馬県高崎市綿貫町1233)

1,2-ビス [(2E, 4E)-オクタデカエイル] -sn-グリセロ-3-ホスホコリン (DODPC) を含有する混合脂質系リポソームの γ 線重合の重合機構解明のため、(a) DODPCと1,2-ジパルミトイル-sn-グリセロ-3-ホスホコリン (DPPC) からなるDODPC/DPPCリポソーム、(b) DODPC, DPPC, コレステロール (Chol), ステアリン酸 (SA) からなるDODPC/DPPC/Chol/SAリポソームの2種類の混合脂質を調製し、 γ 線重合の挙動について調べた。各々の系について、種々のDODPC/DPPCモル比について検討した。また、DODPC/DPPC/Chol/SAリポソームは、リン脂質/Chol/SAのモル比を7/7/2とした。各系のリポソームはエクストルージョン法により孔径 $0.2\mu\text{m}$ のポリカーボネートフィルターを通過させたのち、線量率 3.3kGy/h 、 4°C で γ 線照射により重合を行った。DODPC/DPPCリポソームのモル比5/5、DODPC/DPPC/Chol/SAリポソームのモル比9/1, 8/2, 7/3, 5/5において、重合速度が増加した。重合度は、いずれの系においてもモル比が5/5のときに、DPPCを含有しないDODPCリポソームと比べ増加した。混合脂質リポソームの安定性に関しては、いずれの系もDODPC/DPPCモル比が10/0から8/2までは凍結融解操作に対する粒径変化がなかった。各系のリポソームの γ 線照射による重合挙動を重合速度論的に解析した結果、いずれの系も重合速度の増加が見られたが、重合機構は同じであった。また、DODPCと非重合性成分は、お互いに不溶であることが示唆された。重合速度と重合度の増加は、DPPCまたはコレステロールの疎水性的な相互作用によりDODPCのコンフォメーションが変化し、重合し易いように配向するためと推定された。

(連絡者: 赤間和博・中野善郎) Vol.49, No.6, 591 (2000)

[報文]

ラングミュアープロジェクト膜中での 界面活性アゾ色素の配向： 赤外および紫外可視分光法による研究

今 榮 東洋子^{*1,*2}・鳥居 弘之^{*2}

*1 名古屋大学物質科学国際研究センター

*2 名古屋大学大学院理学研究科

(〒464-8602 愛知県名古屋市千種区不老町)

赤外透過および反射吸収スペクトルが、5および 30mNm^{-1} の表面圧で調製された界面活性アゾ色素のラングミュアープロジェクト (LB) 膜に対して測定された。LB膜内の分子は累積圧に依存して配向することが赤外吸収スペクトルによって示された。紫外可視吸収スペクトルにおいて、トランス配位をとるアゾ色素の吸収帯は 5mNm^{-1} で調製したLB膜ではブルーシフトし、 30mNm^{-1} での膜ではレッドシフトした。これはそれぞれの膜内でHおよびJ会合体が形成されたことを示唆する。LB膜内での界面活性アゾ色素分子の配向が議論された。

(連絡者: 今榮東洋子) Vol.49, No.6, 605 (2000)